11-2011

Spinal Locomotor Inputs to Individually Identified Reticulospinal Neurons in the Lamprey

James T. Buchanan
Marquette University, james.buchanan@marquette.edu

Journal of Neurophysiology, Vol. 106, No. 5 (November 2011): 2346-2357. DOI.

Spinal Locomotor Inputs to Individually Identified Reticulospinal Neurons in The Lamprey

James T. Buchanan
Department of Biological Sciences, Marquette University, Milwaukee, Wisconsin

Abstract

Locomotor feedback signals from the spinal cord to descending brain stem neurons were examined in the lamprey using the uniquely identifiable reticulospinal neurons, the Müller and Mauthner cells. The same identified reticulospinal neurons were recorded in several preparations, under reduced conditions, to address whether an identified reticulospinal neuron shows similar locomotor-related oscillation timing from animal to animal and whether these timing signals can differ significantly from other identified reticulospinal neurons. Intracellular recordings of membrane potential in identified neurons were made in an isolated brain stem-spinal cord preparation with a high-divalent cation solution on the brain stem to suppress indirect neural pathways and with d-glutamate perfusion to the spinal cord to induce fictive swimming. Under these conditions, the

identified reticulospinal neurons show significant clustering of the timings of the peaks and troughs of their locomotor-related oscillations. Whereas most identified neurons oscillated in phase with locomotor bursting in ipsilateral ventral roots of the rostral spinal cord, the B1 Müller cell, which has an ipsilateral descending axon, and the Mauthner cell, which has a contralateral descending axon, both had oscillation peaks that were out of phase with the ipsilateral ventral roots. The differences in oscillation timing appear to be due to differences in synaptic input sources as shown by cross-correlations of fast synaptic activity in pairs of Müller cells. Since the main source of the locomotor input under these experimental conditions is ascending neurons in the spinal cord, these experiments suggest that individual reticulospinal neurons can receive locomotor signals from different subsets of these ascending neurons. This result may indicate that the locomotor feedback signals from the spinal locomotor networks are matched in some way to the motor output functions of the individual reticulospinal neurons, which include command signals for turning and for compensatory movements.

locomotor rhythms in animals are generated by networks of neurons in the central nervous system (Mullins et al. 2011). In vertebrates, the locomotor networks are located within the spinal cord, and these spinal networks are controlled by several systems of descending neurons. These descending systems, especially the reticulospinal system, control various aspects of locomotion such as initiating and terminating locomotion, regulating the speed and direction of locomotion, modifying posture, and maintaining equilibrium (Drew et al. 2008; Dubuc et al. 2008; Matsuyama et al. 2004; Orlovsky et al. 1999; Shaw et al. 2010). The reticulospinal and other descending systems in mammals are informed about the progression of movement and the activity of the locomotor networks by ascending spinal feedback signals that are carried mainly by spinocerebellar neurons (Arshavsky et al. 1972, 1978a, 1978b; Perreault et al. 1993). These rhythmic signals are then conveyed via the cerebellum to the descending neurons (Orlovsky 1970a, 1970b). Our understanding of these three levels of the locomotor system in mammals, i.e., the locomotor networks, the descending control systems, and the ascending feedback systems, is incomplete due to the neural complexities at all three levels. The lamprey, a lower vertebrate, offers a somewhat simpler model system for examining the locomotor system at these three levels. For example, the descending systems in lamprey consist mainly of the reticulospinal and vestibulospinal systems (Ronan 1989; Swain et al. 1993), and the ascending system in lamprey projects more directly to the descending neurons without involving the cerebellum (Einum and Buchanan 2004, 2006; Kasicki et al. 1989; Vinay et al. 1998a). In addition, much is known about the structure and function of the spinal locomotor networks in lamprey including the identity of key component neurons, their electrical properties, and their synaptic interactions (Buchanan 2001; Grillner 2006). Therefore, the lamprey locomotor system provides a simpler and better understood model system for exploring the overall organizational principles of the locomotor system. The present study focuses on the ascending feedback component of the locomotor system that provides information to the reticulospinal neurons regarding the activity of the spinal locomotor networks.

In the lamprey, the ascending signals from the spinal locomotor networks are carried by the spinobulbar neurons. During fictive swimming, these neurons are rhythmically active and show a range of timing patterns in relation to the rhythmic bursting of the adjacent ventral root: whereas many of the spinobulbar neurons are in phase with the ipsilateral ventral root, others are out of phase (Einum and Buchanan 2005). When unidentified reticulospinal neurons were recorded, it was found that they exhibit rhythmic oscillations of their membrane potential that also have a variety of timing patterns in relation to spinal ventral roots: whereas most of the unidentified reticulospinal neurons are in phase with the ipsilateral ventral roots of the rostral spinal cord, about 25% are out of phase (Einum and Buchanan 2005). This finding suggests that the locomotor feedback from the spinal cord may not be the same for all reticulospinal cells and that different reticulospinal neurons receive ascending input from different subsets of spinobulbar neurons.

To test the hypothesis that different reticulospinal neurons receive different ascending locomotor signals, the uniquely identifiable reticulospinal neurons in lamprey were exploited (Buchanan 2001; Rovainen 1967; Zottoli

et al. 2007). By virtue of the size, shape, and position of their cell bodies within the lamprey brain stem, several bilateral pairs of these cells are easily recognized from animal to animal (Fig. 1) so that it is possible to determine the characteristic ascending locomotor inputs to each of these cells. These recordings demonstrate that individually identified reticulospinal neurons have locomotor oscillatory input, due to ascending feedback, that can differ significantly in timing compared with other individually identified reticulospinal neurons. Determining the nature of the ascending locomotor feedback signals to the descending command systems will be important to understanding the functional organization of both the spinal locomotor networks and the descending neurons that control these networks, including understanding how these two levels of the locomotor system interact to produce well-coordinated and directed locomotor movements.

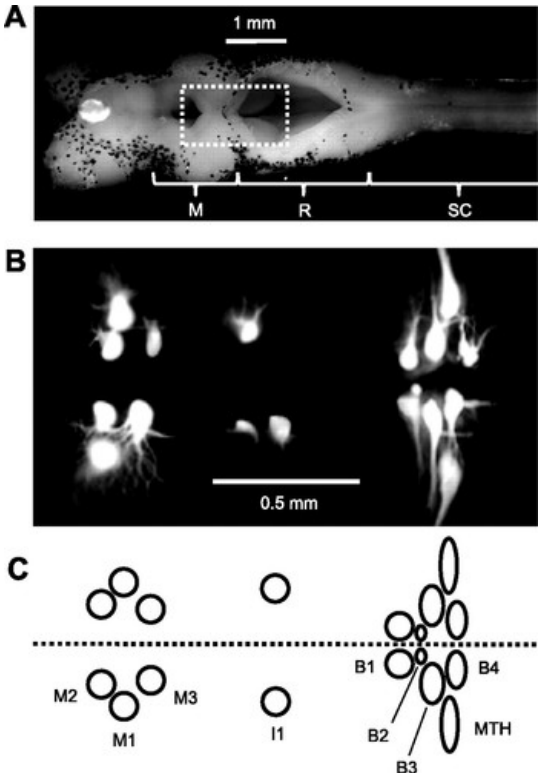

Fig. 1. Locations of the uniquely identifiable Müller and Mauthner cells. *A*: photomicrograph of the dorsal surface of the isolated lamprey (*Petromyzon marinus*) brain and about 2 segments of spinal cord. This brain preparation retains some meningeal sheath that is speckled with numerous dark melanocytes. The dashed rectangle indicates the region shown in *B*. M, mesencephalon; R, rhombencephalon; SC, spinal cord. *B*: fluorescent photomicrograph of Müller and Mauthner cells injected intracellularly with Lucifer yellow. In this image, not all the cells injected were Müller cells and not all Müller cells were successfully injected. The Müller cells not injected were the right I1, right B2, and right B4. The I cell at *right* is I2, as is the smaller I cell at *left*, and the large I cell at *left* is I1. The I2 cells were not used in this study. Two smaller reticulospinal neurons just caudal to the uninjected right B4 were also injected. *C*: schematic of the typical arrangement of the Müller and Mauthner cells used in this study. The dashed line represents the midline. M1–M3, mesencephalic Müller cells located in the mesencephalic reticular nucleus; I1, isthmic Müller cells located in the anterior reticular nucleus; B1–B4, bulbar Müller cells located in the middle rhombencephalic reticular nucleus; MTH, Mauthner cells.

MATERIALS AND METHODS

Animals and dissection.

These experiments were done on 23 adult sea lampreys (*Petromyzon marinus*) that had recently transformed from the larval stage (125–185 mm in length). The animals were obtained from Acme Lamprey (Maine), and

until used for experiments, they were kept in freshwater aquaria at 5°C. The protocols for the experimental procedures and for animal care were approved by the Marquette University Institutional Animal Care and Use Committee.

For dissection, an animal was first anesthetized by immersion in tricaine (250 mg of tricaine per liter of bicarbonate-buffered water) for about 5 min until there was no response to tail pinch. The body was then transected with scissors at the beginning of the dorsal fin in a plane perpendicular to the long axis of the body. After the ventral myotomes, viscera, and oral disk were cut away with scissors, the preparation was transferred to cold Ringer solution (in mM: 91 NaCl, 2.1 KCl, 2.6 $CaCl_2$, 1.8 $MgCl_2$, 4.0 glucose, 20 $NaHCO_3$, 8 HEPES, and 2 Na HEPES, pH 7.4). (Unless noted otherwise, chemicals were obtained from Sigma-Aldrich.) The skin was then cut along its dorsal midline with scissors, and the myotomes were gently pulled away from the notochord. The eyes and head muscles were cut away, and the dorsal fat pad was trimmed off to allow exposure of the spinal cord by making a longitudinal cut along the midline of the cartilage overlying the spinal cord. The brain was then exposed by cutting off the overlying cartilage, and the choroid plexus was removed from the third and fourth ventricles. A transection in a plane perpendicular to the long axis of the brain was made at the rostral border of the mesencephalon to produce a brain stem-spinal cord preparation (Fig. 2*A*). Thus the final preparation consisted of the brain stem attached to the underlying brain case and about 40 segments of spinal cord attached to the underlying notochord. The tissue was kept in cold Ringer solution (4°C) until used for the experiment (within 24 h).

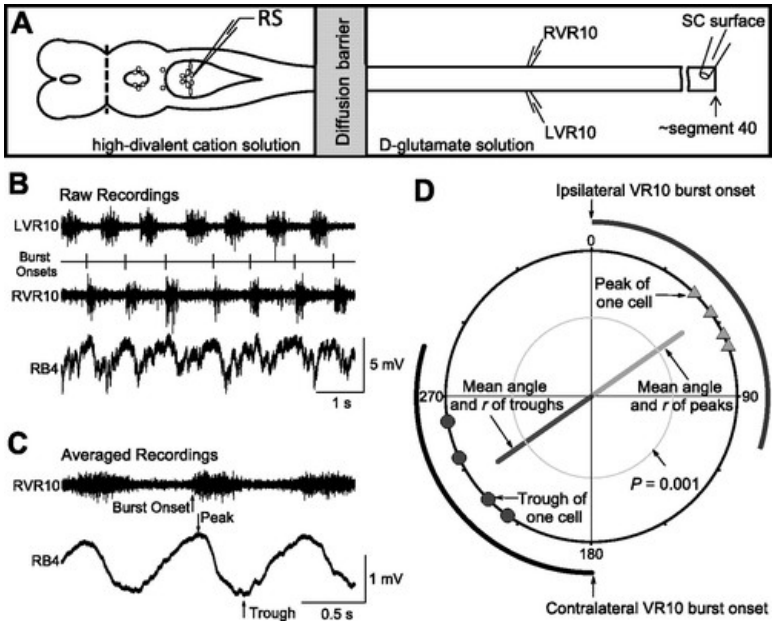

Fig. 2. Experimental configuration and data analysis methods. *A*: brain stem and spinal cord preparation. Although not illustrated, the brain and spinal cord remain attached to the underlying brain case and notochord, respectively. The brain was transected at the rostral border of the mesencephalon as indicated by the dashed line to create a brain stem-spinal cord preparation. The spinal cord extended to the beginning of the dorsal midline fin (to about segment 40 of 100), and a movable surface electrode on the spinal cord near the end was used to record the spikes of reticulospinal axons to determine their laterality and conduction velocity. The laterality of the axons could be determined by moving the suction electrode from one side of the cord to the other and comparing the amplitude of the spikes in an individual axon. Ventral roots on both sides of the spinal cord were recorded at or near segment 10. A petroleum jelly diffusion barrier was constructed at segments 2–4. d-Glutamate (0.7 mM) was added to the spinal cord bath perfusion fluid, and a high-divalent cation solution (20 mM Ca^{2+}, 5.8 mM Mg^{2+}) was added to brain stem bath perfusion. A sharp intracellular microelectrode was used to systematically record the membrane potentials of Müller and Mauthner cells. *B*: a sample of data recorded from the 2 ventral root electrodes and the intracellular electrode in the reticulospinal Müller cell B4.

The onsets of the ventral root bursts ipsilateral to the intracellular somatic recording were marked and used as the trigger signal for the creation of trace averages. *C*: the averaged ipsilateral ventral root bursts and the averaged intracellular recording of the reticulospinal neuron. The timings of the peak and the trough of the averaged oscillation in relation to the onset of the ipsilateral ventral root burst were measured, normalized to cycle period, and expressed as phase angles in degrees. *D:* the phase angles of the peaks (triangles) and troughs (circles) of the same uniquely identified Müller or Mauthner cells recorded in multiple preparations are plotted on a circle. For this circular plot, time progresses clockwise, beginning at the top of the circle at 0°, which is defined as the beginning of the ipsilateral ventral root burst. A typical ipsilateral ventral root burst onset and offset are shown outside the circle as a gray arc; a typical contralateral ventral root burst is shown as a black arc beginning at 180°. The angle of the light gray vector indicates the mean phase angle of the oscillation peaks; the angle of the dark gray vector indicates the mean phase angle of the oscillation troughs. The length of each vector is its *r* value, i.e., the concentration of the individual angles. The gray inner circle is *P* = 0.001 of the Rayleigh *z* value, and it indicates the length of the vector (*r*) needed to provide *P* = 0.001 probability that the data points are not randomly distributed around the circle. RS, reticulospinal neuron; LVR10 and RVR10, ventral root recording at spinal segment number 10 on the left and right sides, respectively; RB4, B4 Müller cell on the right side.

For an experiment, the tissue was transferred to an experimental chamber continuously perfused with cooled Ringer solution (7–9°C), and the tissue was secured to the Sylgard (Dow Corning) floor of the chamber with minutiae pins. As shown in Fig. 1, *A* and *B*, the dorsal roof of the mesencephalon hampers the visibility of and microelectrode access to the rostral Müller cells. Therefore, a dorsal midline cut was made from the third ventricle to the fourth ventricle through the isthmus to improve visibility and access. A petroleum jelly diffusion barrier was constructed around the notochord and spinal cord at spinal segments 2 to 4, dividing the experimental chamber into a brain stem bath and a spinal cord bath with independent fluid perfusion (Fig. 2*A*). Fictive swimming activity was induced in the spinal cord by including 0.7 mM d-glutamate (Tocris) in the spinal cord bath perfusion solution, and the brain stem bath was perfused with a Ringer solution containing elevated Ca^{2+} (20 mM) and elevated Mg^{2+} (5.8 mM). This high-divalent cation solution has been shown in lamprey to reduce polysynaptic pathways with little effect on monosynaptic potentials (Einum and Buchanan 2004).

Recording techniques.

Fictive locomotor activity was recorded by placing the tip of a glass suction electrode onto a ventral root at its exit point from the spinal cord. This was done typically at or near segment 10 on both the left and right sides of the spinal cord (Fig. 2*A*). An additional glass suction electrode was placed on the dorsal surface of the spinal cord near the caudal end of the preparation to record the spikes of reticulospinal axons (Fig. 2*A*). The ventral root signals were amplified (10,000×) and band-pass filtered (100 Hz high pass; 1,000 Hz low pass) with an AM Systems 1700 Differential AC amplifier. The membrane potentials of individual reticulospinal neurons were recorded with sharp intracellular microelectrodes made from thick-walled borosilicate glass capillaries (1 mm outer diameter; World Precision Instruments) pulled on a horizontal puller (P-97; Sutter Instruments) and filled with 4 M potassium acetate. The intracellular signals were recorded with an Axoclamp 2B electrometer (Axon Instruments) and then amplified (50× total) and filtered (3,000 Hz low pass) with a Cyberamp 320 signal conditioner (Axon Instruments). Intracellular signals were digitized to computer with a micro1401 computer interface [Cambridge Electronic Design (CED)] using Spike2 software (CED) at 10,000 Hz. Extracellular signals were digitized at 5,000 Hz.

Cell identification.

Unique reticulospinal neurons (i.e., Müller cells) were recognized by the size, shape, and position of their cell bodies within the brain stem as described by Rovainen (1967) (Fig. 1, *B* and *C*). The following bilateral pairs of Müller cells were used for these experiments: mesencephalic M1, M2, and M3; isthmic I1; and bulbar B1, B2, B3,

and B4. In addition, the bilateral pair of the Mauthner cell (Fig. 1, *B* and *C*) with its contralateral axonal projection was also included in the study. The cells were generally easily visualized with a stereomicroscope (Wild M5A) without labeling, but on occasion they were injected with Lucifer yellow CH (5% in 1 M LiCl) from an intracellular microelectrode using pressure (Picrospritzer II; General Valve) at the end of the experiment for later confirmation. After injection, the tissue was fixed by immersion in cold 10% neutral buffered formalin for at least 2 h and then washed in Ringer solution, dehydrated in an ethanol series, and cleared by immersion in methyl salicylate. The whole brain stem was mounted on a depression slide in methyl salicylate, viewed with an epifluorescence microscope (Nikon E-600), photographed with a digital camera (Spot; Diagnostic Instruments). In addition to the shape, size, and location of the cell body, the axon conduction velocity was measured with the caudal spinal cord recording to help confirm the identity of the neurons. Müller and Mauthner axons project long distances down the spinal cord, well beyond the location of the extracellular electrode used to record their axon spikes (Fig. 2*A*). The Müller and Mauthner cells had conduction velocities >3 m/s (typically 3.2–4.0 m/s) except for the B2 Müller cell, which had conduction velocities <3 m/s (typically 1.2–2.2 m/s). The Mauthner cells were further tested for laterality of their axon in the spinal cord by moving the suction electrode from one side of the cord to the other and comparing the amplitude of spikes of an individual axon. After somatic impalement and stabilization of the membrane potential, an identified Müller or Mauthner cell was recorded during fictive swimming for about 5 min. Only cells with membrane potentials of at least −65 mV were used in the analysis, assessed by removing the microelectrode from the cell and correcting for any electrode offset.

Data analysis.

The timing of the membrane potential oscillations in the reticulospinal neurons in relation to the ipsilateral ventral root bursting was determined. For this analysis, averages of the intracellular and extracellular signals were created using ipsilateral ventral root burst onsets as the trigger for the averages (Fig. 2, *B* and *C*). To mark burst onsets, the ventral root bursts were transformed into rectified burst envelopes using a digital filter with a 50-ms time constant (script provided by CED). The burst onsets were then automatically marked using Spike2 software by setting a voltage detection threshold above the background noise. The accuracy of this automatic detection of bursts was manually checked and corrected when necessary. The resulting event times were used to trigger an average of the raw ventral root bursts and an average of the intracellular recording of the reticulospinal neuron (Fig. 2*C*). Typically, about 200 consecutive swim cycles were used for the averages. The times of occurrence of the peak and the trough of the averaged intracellular oscillation with respect to the onset of the averaged ventral root burst were measured (Fig. 2*C*) and normalized to the mean cycle period (the mean of the event time intervals). In most cases the oscillation waveform had a clear peak and trough. If the oscillation waveform had a broad peak or broad trough, the midpoint of the peak or trough was estimated by eye. These normalized timings are referred to as the peak phase angle and the trough phase angle and are expressed in degrees. For each identified neuron, the phase angles were plotted on a circular plot where time proceeds clockwise, and the ipsilateral ventral root burst begins at the top of the circle at 0° (Fig. 2*D*). The amplitude of the oscillations was measured as the peak-to-trough amplitude of the averaged oscillation. The phases are expressed in relation to the 10th spinal segment ventral root by making a correction of 1% of a cycle period for each segment of deviation from segment 10 to where the actual ventral root recording was made (between segment 10 and segment 17). When membrane potential oscillations in a cell exhibited two depolarizing peaks per swim cycle, the larger peak and trough were used for measuring the peak and trough phase angles.

In some experiments, intracellular recordings were made from two Müller cells simultaneously to measure the cross-correlation of synaptic inputs to the cell pairs during fictive swimming using methods previously described (Buchanan and Kasicki 1999). For these experiments, a grounded aluminum foil shield was placed between the two microelectrodes and their holders to reduce inter-electrode artifacts. The signals were recorded on a digital audio tape recorder (Biologic) and digitized later for analysis. The slow swim oscillations were removed with a

digital notch filter (script provided by CED). Waveform cross-correlation was then performed on the two simultaneously recorded intracellular signals for 50 swim cycles using Spike2 software (CED). The amplitude of the peak of the cross-correlation function was used as a measure of the degree of correlation of fast synaptic activity.

Pharmacology.

To test the pharmacology of the locomotor inputs to the Müller cells, neurotransmitter antagonists were added to the perfusion fluid of the brain stem bath: strychnine (5 μM) to antagonize glycine receptors and kynurenic acid (2 mM) to antagonize ionotropic glutamate receptors. These drugs were used either alone or in combination and were perfused into the brain stem bath for at least 30 min at rates of 0.5 to 1 bath exchange per minute. Kynurenic acid was added first, and then once the effect of kynurenic acid had reached a steady state, strychnine was added.

Statistics.

For each identified reticulospinal neuron, circular statistics (Zar 1999) were used to calculate the mean phase angles for the peaks and the troughs of the intracellular oscillations recorded in cells from several animals. The mean phase angle and the *r* value of the mean are represented on the circular plots as a vector (Fig. 2*D*). The Rayleigh test was used to determine whether the phase angles for the peaks and troughs for each identified cell had a nonrandom distribution. A gray circle is drawn on each cell's circular plot to indicate the value of *r* required for a nonrandom distribution at the $P = 0.001$ level based on the Rayleigh test (Zar 1999) (Fig. 2*D*). To test whether the phase angles of pairs of identified reticulospinal cells were significantly different, the nonparametric Wheeler and Watson test was used, rather than a parametric test, due to the irregular distribution of values in some cells ($P < 0.001$ for significance) (Zar 1999). For the pharmacology experiments, paired *t*-tests were used to test the significance at the $P < 0.05$ level. For the oscillation amplitude measurements, a nonparametric one-way ANOVA was used (Kruskal-Wallis) with a Dunn's multiple comparison test ($P < 0.05$). For the cross-correlation experiments, a *t*-test was used ($P < 0.05$).

RESULTS

Oscillation shapes and amplitudes.

The uniquely identified reticulospinal Müller and Mauthner cells exhibited membrane potential oscillations during fictive swimming in the spinal cord. Since these oscillations occurred in the presence of high-divalent cation solution in the brain stem bath, they likely result from direct synaptic inputs from ascending spinal neurons. The oscillations in Müller and Mauthner cells had a variety of shapes (Fig. 3). Typically the oscillations had a single peak and trough, either with or without an inflection on the rising or falling phase (70% of all 157 cells) (Fig. 3*A*). Many cells, however, exhibited two peaks per swim cycle separated by a second trough (30% of all cells). In the case of double peaks, one of the peaks was usually larger (27% of all cells) (Fig. 3*B*), although rarely the two peaks were nearly equal in size (3% of all cells) (Fig. 3*C*). On average, the two peaks occurring in a cell had a separation of about one-half of a swim cycle (mean = 173°; Fig. 3*D*). Although each of the different Müller and Mauthner cells could show double peaks, the I1 Müller cell had the smallest fraction of cells with double peaks (1 of 19), whereas B1 had the largest fraction (12 of 18). Nearly every brain stem preparation showed at least one cell with a double peak, whereas in several preparations, nearly every cell exhibited double peaks. The presence of double peaks in the oscillations indicates that spinal locomotor inputs to reticulospinal neurons are not simply a duplicate of ipsilateral motoneuron activity, since lamprey spinal motoneurons do not exhibit double peaks (Buchanan and Cohen 1982; Buchanan and Kasicki 1995; Wallén et al. 1985).

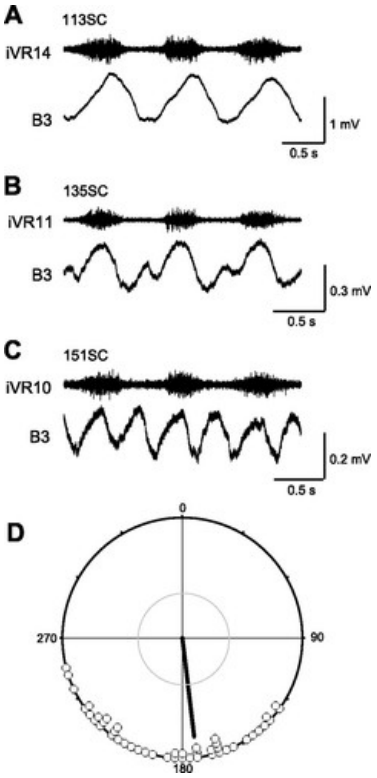

Fig. 3. Examples of averaged waveforms of locomotor oscillations observed in a single Müller cell (B3) in 3 different preparations (labeled with identifying preparation numbers). *A*: the oscillations could be simple with a single peak and trough, with or without an inflection. *B*: in some cases, there could be double peaks and troughs, usually with 1 peak being much smaller than the other. *C*: in rare cases, the double peaks were of similar size. *D*: a plot of the phase difference between the double peaks reveals that the 2 peaks tend to occur at about one-half swim cycle apart (173°). For this plot, the time between the 2 peaks was measured in trace averages, normalized to cycle period, and expressed as degrees. These data comprise 47 cells with double peaks from 17 preparations. iVR, ipsilateral ventral root recording at the spinal segment number indicated.

The locomotor oscillations in Müller and Mauthner cells were small in amplitude and always below spike threshold. The amplitudes of the oscillations were generally related to the rostrocaudal position of the cell: the rostrally located M cells had smaller oscillation amplitudes than the caudally located B cells (Fig. 4). This trend is consistent with a previous anatomical demonstration that spinobulbar projections become less dense with distance from the spinal cord, ending in the caudal mesencephalon (Ronan and Northcutt 1990).

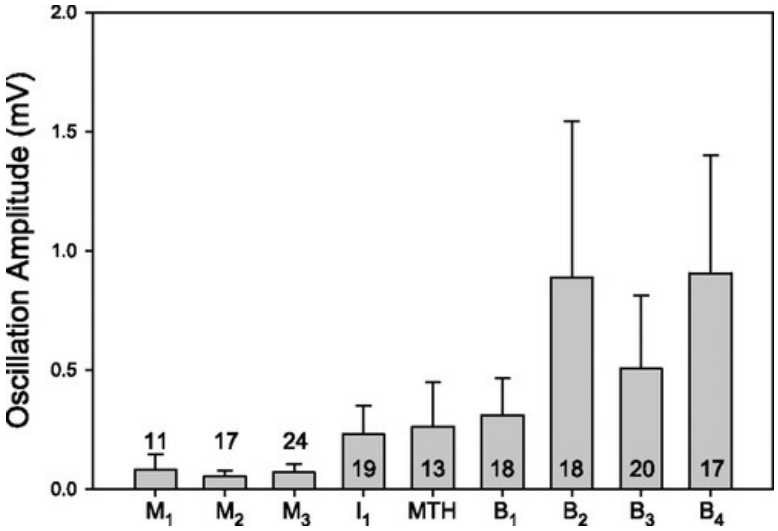

Fig. 4. Mean peak-to-trough amplitudes of the locomotor oscillations in the Müller and Mauthner cells. Generally, the closer the cell's location to the spinal cord, the larger the amplitudes. Bar height is the mean oscillation amplitude of the population, and the error bar is +SD. The B2–B4 amplitudes are significantly larger than M1–M3 amplitudes ($P < 0.05$, Kruskal-Wallis 1-way ANOVA, Dunn's test for multiple comparisons). The number of cells in each group is indicated by the number in or above each bar.

Oscillation pharmacology.

The B1–B4 Müller cells were used to examine the pharmacology of the locomotor synaptic inputs. Application of kynurenic acid (2 mM), a nonselective blocker of ionotropic glutamate receptors, reduced the peak-to-trough oscillation amplitude in each cell tested, presumably by blocking excitatory glutamatergic synaptic inputs from the spinal cord. As shown in Fig. 5, *A1* and *A2*, kynurenic acid did not affect the maximum value of the troughs but reduced the maximum of the peaks (note membrane potential reference line at *right*). On average, kynurenic acid application reduced the oscillation amplitude to 60% of the control value ($n = 10$ cells; $P = 0.004$, paired *t*-test) (Fig. 5*B1*). To test the contribution of glycinergic inhibition to the locomotor oscillations, strychnine (5 μM), an antagonist of glycine, was added to the brain stem bath, with or without kynurenic acid present. When kynurenic acid was present, the strychnine was not added until the effect of kynurenic acid had reached a steady state. An example is shown in Fig. 5, *A2* and *A3*, in which kynurenic acid was present when strychnine was added, and strychnine further reduced the oscillation amplitude by reducing the maximum amplitude of the troughs. When strychnine was added either alone ($n = 2$) or in the presence of kynurenic acid ($n = 6$), the amplitude of the oscillations was reduced in every cell tested. On average, strychnine reduced the oscillation amplitudes to 45% of the value preceding strychnine application ($n = 8$ cells; $P = 0.04$, paired *t*-test) (Fig. 5*B2*).

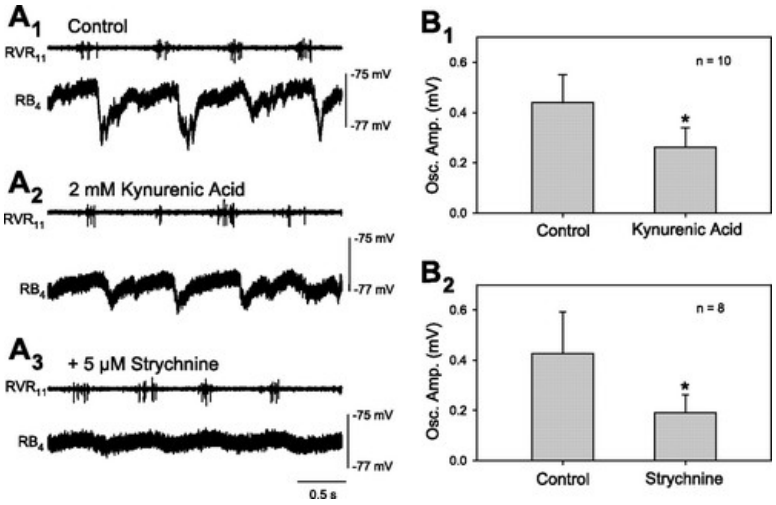

Fig. 5. Test of the pharmacology of the locomotor oscillations in Müller cells. *A*: raw traces illustrate a B4 neuron exposed first to kynurenic acid in the brain stem bathing solution (*A2*), producing a reduction in the maximum amplitude of the depolarizing phase of the oscillations with little effect on the maximum level of the trough compared with control (*A1*). Strychnine was added after the effects of kynurenic acid had reached a steady state (*A3*), resulting in a further decrease in oscillation amplitude by reducing the maximum level of the troughs. The calibration bars at *right* indicate the membrane potential. *B*: summary of blocker effects. Kynurenic acid (2 mM; *B1*) and strychnine (5 µM; *B2*) significantly reduced oscillation amplitude (**P* < 0.05 vs. control, paired *t*-test). The experiments were done on a mixture of all of the B Müller cells. Strychnine was often (*n* = 6), but not always (*n* = 2), applied in the presence of kynurenic acid. Control is the amplitude of oscillations just before the drug is introduced. Osc. Amp., oscillation amplitude.

Oscillation timing.

To address whether individual reticulospinal neurons receive different spinal locomotor inputs than other individual reticulospinal neurons, the timings of the oscillation peaks and troughs were used as indicators of ascending spinal signals. An example of the timings of the peaks and troughs observed in several cells in one preparation is shown in Fig. 6. Several cells have different timings of their peaks and troughs of the averaged oscillation waveform compared with the other cells, notably the peaks of the B1 and the Mauthner cell and the troughs of I1, M3, and the Mauthner cell. To determine whether such differences are a characteristic feature of the cells, recordings were made from the same Müller and Mauthner cells in several preparations. Circular statistics were used to determine whether any of the uniquely identified reticulospinal neurons recorded in several preparations had significantly different timings of their oscillations compared with other cells. For each identified cell, the distributions of both their peak and trough phase angles in all the preparations were nonrandom as shown by the *r* value of the mean phase angle (i.e., vector length) exceeding the value of the inner circle, which is the *P* = 0.001 level for a nonrandom distribution (see Figs. 7, 9, and 10).

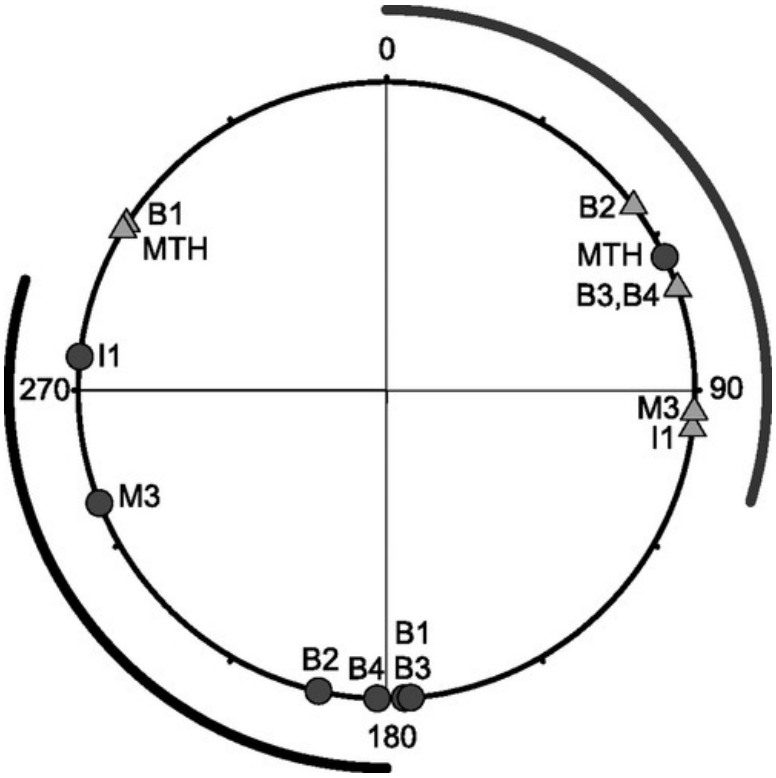

Fig. 6. Examples of peak and trough timings of several identified Müller and Mauthner cells recorded in the same preparation (127SC). Some of the cells showed different timings of the peak and trough of their averaged locomotor oscillation from the spinal cord, suggesting that some of the individual cells are receiving different ascending inputs.

The results for the three Müller cells of the mesencephalic reticular nucleus (M1, M2, and M3) are shown in Fig. 7. The circular plot of the oscillation peaks and troughs are shown for each of the Müller cells, and three examples of individual cells are shown below the circular plot. The mean phase angles for peaks and troughs were similar for the three M cells with the mean peak angle coming near the end of the ipsilateral ventral root burst and the mean trough angle coming near the middle of the contralateral ventral root burst. These phase angles were not significantly different from one another at the $P < 0.001$ level (Wheeler and Watson test) (Fig. 8). However, the M cells did show significant differences with the Mauthner cell and the B1 Müller cell, and the trough angles of M3 were significantly different from several other cells (Fig. 8).

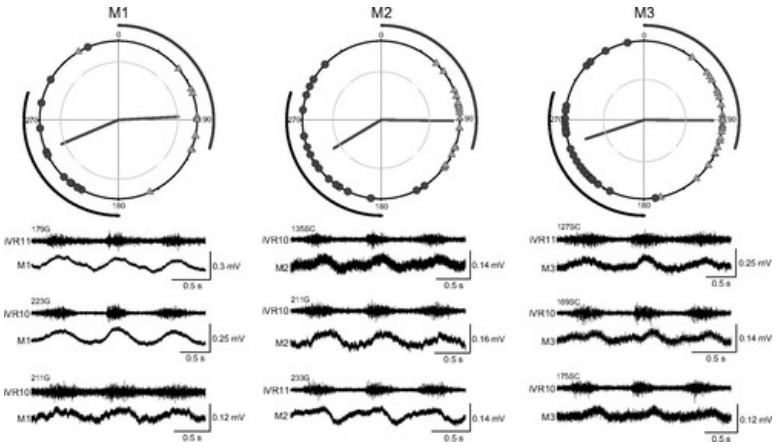

Fig. 7. Summary of oscillation timings in M1, M2, and M3 Müller cells. *Top*: circular plots showing the phase angles of the peak (triangles) and trough (circles) for each of the cells recorded. The vectors in the circular plots

give the mean phase angle for the peaks (light gray) and the troughs (dark gray). The length of the vector is *r*, a measure of the concentration of the phase angles. The inner circle indicates the *r* value required to reject the hypothesis that the angles are randomly distributed on the circle (*P* = 0.001). *Bottom*: 3 representative traces for each of the Müller cells, recorded in different preparations (identifying preparation number given for each trace). Number of cells in each plot: M1 = 11; M2 = 17; M3 = 24.

	M1	M2	M3	I1	Mth	B1	B2	B3	B4
M1	–				PT	PT			
M2		--			PT	PT			
M3			–	T	PT	PT		T	T
I1			T	--	PT	PT	T		PT
Mth	PT	PT	PT	PT	--	T	PT	PT	PT
B1	PT	PT	PT	PT	T	--	P	P	P
B2				T	PT	P	--		
B3			T		PT	P		–	
B4			T	PT	PT	P			--

Fig. 8. Summary of significant differences in the oscillation timings between the recorded populations of each Müller and Mauthner cell using a nonparametric test of circular statistics (Wheeler and Watson test) between pairs of populations. In this matrix, a significant difference in the timing of the peaks (P), troughs (T), or both (PT) is indicated by the presence the corresponding letter (*P* < 0.001).

In Fig. 9, the I1 and B1 Müller cells are shown along with the Mauthner cell. These three cells show significant differences in the timings of their locomotor oscillations compared with other cells. For example, the troughs of the oscillations of the I1 cells tend to occur later in the locomotor cycle, and the mean of the trough phase angles was significantly different from that of several other cell types (Fig. 8). The Mauthner cell and the B1 Müller cell have out-of-phase peaks that occur near the end of the contralateral ventral root burst, rather than during the ipsilateral ventral root burst as observed in most other cells. The mean peak phase angles of the Mauthner and B1 cells were significantly different from those of all other cells (Fig. 8). The remaining B cells (B2, B3, and B4) had peak and trough timings (Fig. 10) that were not significantly different from one another but showed significant differences from some other cells (Fig. 8).

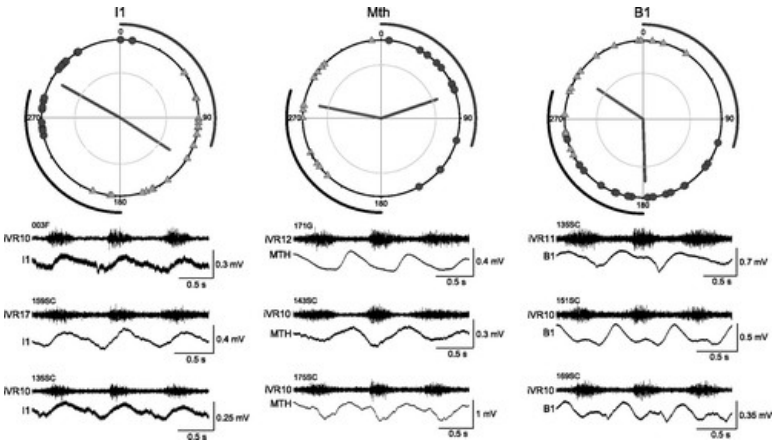

Fig. 9. Summary of the oscillation timings in I1, Mauthner, and B1 cells. These 3 cells have differences in the timings of their peaks and troughs compared with other cells. For example, the means of the peak phase angles of B1 Müller cell and the Mauthner cell differ from the peaks of all other cells, because they tend to occur near the end of the contralateral ventral root burst instead of during the ipsilateral ventral root burst as in most cells. Number of cells in each plot: I1 = 19; Mauthner = 13; B1 = 18.

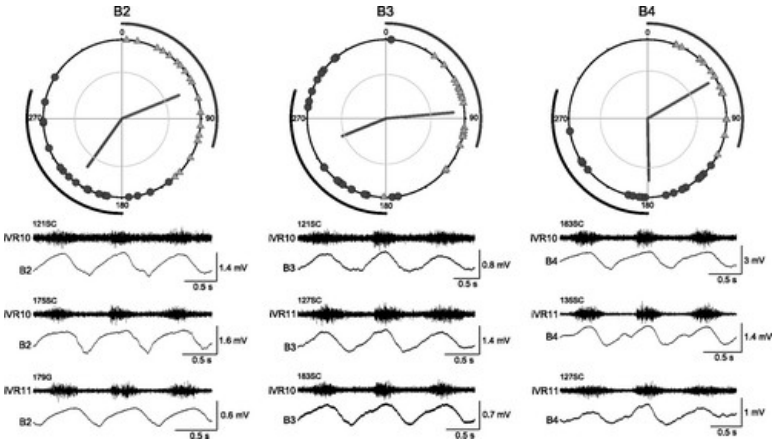

Fig. 10. Summary of the oscillation timings in B2, B3, and B4 cells. These Müller cells tend to have larger amplitude oscillations than the other Müller cells and the Mauthner cells. The mean phase angles of the peaks and troughs are not significantly different from one another but do have significant differences with other cells. Number of cells in each plot: B2 = 18; B3 = 20; B4 = 17.

Cross-correlation of synaptic activity.

One explanation for the differences in oscillation timings is that cells with different timings receive synaptic inputs from different sets of ascending neurons. To test this hypothesis, simultaneous intracellular recordings were made between ipsilateral pairs of the B cells using the same experimental set up shown in Fig. 2*A*. The B Müller cells were used for this analysis because of their close proximity to one another (Fig. 1) and because the B1 Müller cell has significant differences in oscillation timing compared with B2, B3, and B4 Müller cells (Fig. 8). Examples of raw traces from paired recordings are shown in Fig. 11*A*. Simultaneous recording of B2 and B4 on the same side (Fig. 11*Ai*) showed many synchronous synaptic inputs, but when B1 and B4 were recorded together, there was little similarity in their synaptic inputs (Fig. 11*Aii*). A recording with two electrodes in the same B4 neuron is illustrated in Fig. 11*Aiii*.

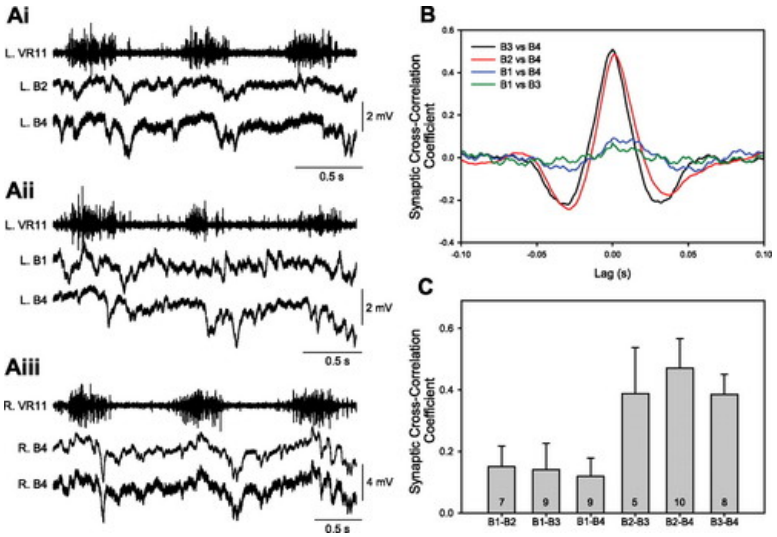

Fig. 11. Cross-correlations of fast synaptic activity between pairs of B cells. *A*: examples of raw traces from simultaneous intracellular recordings of pairs of ipsilateral B cells in 1 preparation (233G): *i*, paired recording of B2 and B4 on the same side (peak cross-correlation coefficient = 0.50); *ii*, paired recording of B1 and B4 on the same side (peak cross-correlation coefficient = 0.08); *iii*, dual impalement of B4 (peak cross-correlation coefficient = 0.92). *B*: examples of the cross-correlations in another preparation (135SC) showing that B1 vs. B3

or B4 had low correlation coefficients, whereas B4 vs. B3 or B2 had higher correlation coefficients. *C*: this same pattern was observed in several preparations, and the means (+SD) are summarized in the bars. The fast synaptic activity of B1 had low correlation when paired with B2, B3, or B4, whereas pairs among B2, B3, and B4 had significantly higher correlations than pairs involving B1 ($P < 0.05$, *t*-test). The number in each bar indicates the number of paired recordings performed.

To quantify the degree of common synaptic inputs during fictive swimming, the swim oscillation frequency was digitally removed and waveform cross-correlations were then performed between pairs of ipsilateral B cells. Examples of cross-correlations of the fast synaptic activity are shown in Fig. 11*B*, and a summary of all pairings is shown in Fig. 11*C*. There is a higher cross-correlation coefficient between pairings of B2, B3, and B4 cells (range of means = 0.39 to 0.47) compared with the cross-correlation coefficient between pairings of B1 with the B2, B3, and B4 cells (range of means = 0.12 to 0.15) ($P < 0.05$, *t*-test). When both electrodes were placed into the same B4 cell, the mean cross-correlation coefficient was 0.93 ± 0.05 ($n = 3$ cells), demonstrating that the correlation differences are not due to differences in electrode properties. Thus the differences in correlation of synaptic inputs suggest that the differences in oscillation timings can be attributed to differences in the neuronal sources of synaptic inputs.

DISCUSSION

These experiments demonstrate that the locomotor oscillations recorded in uniquely identifiable Müller and Mauthner reticulospinal neurons of the lamprey have different timings among the identified neurons. Since the reticulospinal neurons were recorded in the presence of high-divalent cation solution, the locomotor inputs were largely direct from the spinal cord. The differences in timings of the locomotor signals were therefore likely due to differences in the distribution of ascending spinal locomotor signals among the reticulospinal neurons. This conclusion was supported by the demonstration of higher cross-correlations of fast synaptic activity between pairs of reticulospinal neurons that have similar locomotor oscillation timings compared with pairs of reticulospinal neurons that have different timings. These findings suggest that individual reticulospinal neurons receive locomotor inputs from different subsets of ascending spinobulbar neurons, perhaps signaling the activities of different components of the spinal locomotor networks.

The Müller and Mauthner cells appear to be involved in the control of locomotor activity in lamprey. During electrical stimulus-induced episodes of fictive swimming in the isolated brain stem-spinal cord preparation, Müller and Mauthner cells exhibit strong depolarizations and rhythmic firing lasting for the duration of the swim episode (Fagerstedt et al. 2001; Kasicki et al. 1989). During fictive turning, larger reticulospinal neurons including the Müller cells exhibit modulation of their firing depending on the direction of the turn (Fagerstedt et al. 2001). Recordings of reticulospinal axons in intact, freely swimming lampreys revealed that the larger reticulospinal neurons (those with conduction velocities between 2.5 and 5 m/s) exhibit changes in firing rates during swim initiation and termination and during changes in swim intensity, turning, and equilibrium compensation (Deliagina et al. 2000). Based on the conduction velocities, these recordings likely included Müller cell axons. There is much stronger evidence that smaller reticulospinal neurons contribute to the control of locomotion as shown by the preservation of descending locomotor control after most Müller axons were cut by a transverse midline lesion in the rostral spinal cord (Shaw et al. 2010). The axons of most small reticulospinal neurons project more laterally than the Müller cells and for shorter distances. The Müller cells project nearly the full length of the spinal cord (Swain et al. 1993).

The uniquely identifiable Müller and Mauthner cells appear to be similar to other reticulospinal neurons with respect to their locomotor input from the spinal cord and may, therefore, be considered as representative of the reticulospinal neurons. Previous studies using a similar preparation of the lamprey brain stem and spinal cord

used randomly impaled reticulospinal neurons including cells of the posterior rhombencephalic reticular nucleus, which lacks identifiable reticulospinal cells (Einum and Buchanan 2004, 2005). The similarities between the non-Müller and the Müller reticulospinal neurons include the amplitudes of the oscillations, the range of oscillation timing, and the pharmacology of the oscillations. Both the previous and the current studies found that reticulospinal neurons receive spinal locomotor signals consisting of excitatory and inhibitory synaptic inputs. The earlier study with nonidentified reticulospinal cells (Einum and Buchanan 2004) demonstrated a reduction of the inhibitory component with strychnine, leaving a depolarizing component that was presumed to be glutamatergic excitation. The present study used the B Müller cells to confirm that the inhibitory component is reduced by strychnine and to further show that the depolarizing component is reduced by kynurenic acid and therefore is glutamatergic.

The locomotor oscillations reported in the current study are likely due to direct inputs to the identified reticulospinal neurons from spinobulbar neurons, because they were recorded while the brain stem was bathed in a high-divalent cation solution. This solution raises spike threshold and thus reduces the likelihood that indirect pathways will be active (Berry and Pentreath 1976). A previous study demonstrated in lamprey that the combination of elevated Ca^{2+} and elevated Mg^{2+} used in the current study produces a large reduction in polysynaptic postsynaptic potentials with little change in monosynaptic postsynaptic potentials (Einum and Buchanan 2004). This previous study also showed that the locomotor oscillations in nonidentified reticulospinal neurons did not change significantly when the high-divalent cation solution was added after the oscillations were first recorded in normal solution, showing that even in the absence of the high-divalent cation solution, the locomotor inputs to the reticulospinal neurons are largely direct from the spinal cord. Paired intracellular recordings have further shown that monosynaptic interactions from spinobulbar neurons to reticulospinal neurons exist and that these interactions can be either excitatory or inhibitory. Both the excitatory and the inhibitory spinobulbar neurons can project either ipsilaterally or contralaterally to the brain stem (Einum and Buchanan 2006). Although direct inputs clearly exist, indirect inputs to reticulospinal neurons cannot be completely ruled out, even in the presence of high-divalent cation solution. However, given the existence of direct inputs shown with paired recordings and given the low amplitude of the oscillations, it is likely that the locomotor inputs observed in the current study are produced by direct synaptic input to the identified reticulospinal neurons from spinobulbar neurons.

The amplitude of the oscillations observed in the current study for identified reticulospinal neurons were small and always subthreshold for spiking. The amplitudes of the oscillations were found to be largest in those Müller cells closest to the spinal cord (B cells) and smallest in those furthest from the spinal cord (M cells). This finding is consistent with the results of an anatomical study (Ronan and Northcutt 1990) that examined the distribution of spinobulbar axons by using a silver stain for degenerating axons following spinal hemisection and which found that ascending axons extended as far as the caudal mesencephalon.

The small amplitude of the oscillations observed in the present study and in previous studies (Dubuc and Grillner 1989; Einum and Buchanan 2004, 2005) is in contrast to the situation in normal physiological solution when swimming activity is initiated by the brain stem rather than by bathing the spinal cord with an excitatory amino acid (Di Prisco et al. 1997; Kasicki and Grillner 1986; Kasicki et al. 1989). In brain stem-induced fictive swimming, the oscillations in reticulospinal neurons (Müller and non-Müller) are much larger in amplitude and can produce rhythmic modulation of spiking of the reticulospinal neuron. Blockage of ascending spinal inputs during brain stem-induced swimming using local Xylocaine application to the rostral spinal cord significantly reduced the duration of the depolarizations associated with swimming and eliminated the oscillations in nonidentified reticulospinal neurons, indicating that the ascending input from the spinal cord plays a significant role in the reticulospinal neuron activity during swimming activity (Antri et al. 2009). The small amplitudes of the ascending locomotor inputs observed under the conditions of the current experiments likely were a major contributing

factor to the variation in the timing of inputs from preparation to preparation for the same identified reticulospinal cell. The small amplitude of the inputs necessitated averaging of the signals, and variations in cycle-to-cycle durations occurring during the sequence of swimming used for averaging would lead to a degradation of the timing signals in the average. In addition, the averaged locomotor oscillations in the neurons could have rather broad peaks and troughs, introducing variability in the measurement of a single time points for the peak and the trough.

There are several possibilities to account for the differences in amplitude of the locomotor signals in brain stem-induced locomotor activity compared with bath glutamate-induced locomotor activity. First, it is known that the swimming activity generated by the brain stem produces 50–100% larger oscillation amplitudes in spinal motoneurons and interneurons than occurs in the isolated spinal cord when swimming activity is induced by bath-applied glutamate (Buchanan and Kasicki 1995). If spinobulbar neurons are also more strongly activated during brain stem-induced locomotor activity, they would provide a stronger feedback to reticulospinal neurons compared with glutamate-induced swimming activity. Mutual excitatory coupling among reticulospinal neurons has been shown in *Xenopus* tadpoles (Li et al. 2006, 2009) and, if present in lamprey, would enhance brain stem-induced activity. Mutual excitation between reticulospinal neurons and some excitatory spinobulbar neurons has been shown in lamprey (Einum and Buchanan 2006). Second, the density of spinobulbar neurons is highest in the most rostral spinal segments and falls sharply with distance from the brain stem (Vinay et al. 1998b). The diffusion barrier in the current study was placed over segments 2 to 4 so that the region of highest spinobulbar neuron density is not being activated by the glutamate solution. This would be expected to result in weaker inputs to the reticulospinal neurons compared with full activation of spinobulbar neurons. Third, during brain stem-induced locomotion there is a large depolarization of the reticulospinal neurons. This depolarization appears to be a combination of input from within the brain stem (Brocard et al. 2010; Di Prisco et al. 1997; Smetana et al. 2010), intrinsic properties of the cells (Di Prisco et al. 2000), and spinal inputs (Antri et al. 2009). Rhythmic inputs from the spinal cord, especially inhibitory ones, may be more effective at sculpting out oscillations from this depolarized plateau than similar inputs to otherwise quiescent cells. There is also evidence that the brain stem itself can generate rhythmic locomotor activity in lamprey (Jackson et al. 2005) as well as in *Xenopus* tadpoles (Soffe et al. 2009) and in larval zebrafish (Chong and Drapeau 2007).

In the present studies, all of the Müller cells and the Mauthner cells could exhibit double peaks in their oscillations during each swim cycle. Double peaks are also apparent in reticulospinal neurons during fictive swimming induced by brief electrical stimulation of the spinal cord (Kasicki and Grillner 1986; Kasicki et al. 1989). Double peaks are not observed in motoneurons during fictive locomotion (Buchanan and Cohen 1982; Buchanan and Kasicki 1995; Wallén et al. 1985). Considering that the two peaks occur about one-half swim cycle apart, it seems likely that the out-of-phase peak results from input from the contralateral locomotor networks in the spinal cord. Another possible source of the out-of-phase peak could be ipsilateral networks located at a caudal distance sufficient to produce a 50% lag in activity, i.e., ~50 spinal segments (Wallén and Williams 1984). The preparations used in the present study had about 35 active spinal segments, so although it is possible that the caudal end of the spinal cord preparation could be sufficiently delayed to be consistent with the out-of-phase peak, this possibility is unlikely due to the low density of spinobulbar neurons at this distance from the brain stem (Vinay et al. 1998b). The likeliest explanation is that all of the oscillations originate mainly from the most rostral spinal segments, where there is the highest density of spinobulbar neurons, and the out-of-phase peaks represent input from the locomotor networks on the opposite side of the spinal cord. Since in the rostral spinal cord both ipsilateral and contralateral ascending spinobulbar neurons exist (Einum and Buchanan 2006; Vinay et al. 1998b), can be either excitatory or inhibitory, and are rhythmically active during locomotion (Einum and Buchanan 2006), the anatomical substrate exists for input to reticulospinal neurons from the contralateral locomotor networks. The amplitude of the out-of-phase peak could be quite variable in the same identified neuron from preparation to preparation. Whether this variability is due to differences in the

brain stem (e.g., perhaps the same ascending inputs could be filtered by presynaptic inhibitory mechanisms to different degrees in different preparations) or to differences in the ascending neuron activity in the spinal cord is unknown.

The main result of the present study is that some identified reticulospinal neurons have oscillation patterns that are significantly different from that of other identified reticulospinal neurons. This was suggested in a previous study of randomly impaled reticulospinal neurons where it was found that about 25% of the nonidentified reticulospinal neurons oscillated out of phase with the ipsilateral ventral root (Einum and Buchanan 2005). The present study was undertaken to determine whether such differences constitute characteristic differences in particular cells. Using the uniquely identified Müller cells and the Mauthner cells, we found that significant differences do exist among these cells. One of the out-of-phase cells recorded in the current study was the Mauthner cell. This antiphasic activity has been observed previously in brain stem-initiated fictive swimming (Kasicki and Grillner 1986) and is consistent with its contralaterally projecting axon. In addition to the Mauthner cell, the B1 Müller cell was found in this study to also oscillate in phase with the contralateral ventral roots. However, unlike the Mauthner cell, the B1 cell has an ipsilateral descending axon (Rovainen 1967). The B1 is different from most other Müller cells in that it does not excite motoneurons (Rovainen 1974) but rather provides indirect inhibition to motoneurons (Buchanan 1982). Although the other Müller cells generally had oscillations in phase with the ipsilateral ventral root, there were significant differences among them, in the timing of either their oscillation peak or trough, or both. For example, I1 was significantly different from 5 of the other 8 cells in the timing of its oscillations.

Presumably the ascending locomotor signals to the reticulospinal cells serve to adjust the timing of the reticulospinal cell output spiking during swimming. Thus it appears likely that the differences in these spinal inputs to reticulospinal neurons may be related to the outputs of the reticulospinal neurons in the spinal cord. It is known that individual reticulospinal neurons have distinctive output patterns to different classes of spinal neurons (Buchanan 1982, 2001; Rovainen 1974). In addition, stimulation of individual reticulospinal neurons during fictive swimming produces different effects on motoneuron firing depending on the body quadrant the motoneuron innervates (Zelenin et al. 2001), and vestibular inputs to an individual reticulospinal neuron can match well that neuron's motor output pattern (Zelenin et al. 2007). We propose that the spinal inputs to individual reticulospinal neurons may also be matched in some way to the output patterns of individual reticulospinal cells. The functional relationship of spinal locomotor inputs to reticulospinal outputs remains to be determined, but by using the uniquely identified reticulospinal neurons, this relationship may be revealed.

GRANTS

This work was supported by National Institute of Neurological Disorders and Stroke Grant NS-40755.

DISCLOSURES

No conflicts of interest, financial or otherwise, are declared by the author(s).

ACKNOWLEDGMENTS

The assistance of Doris Kim and Zain Syed in some of these experiments is gratefully acknowledged.

AUTHOR NOTES

- Address for reprint requests and other correspondence: J. T. Buchanan, Dept. of Biological Sciences, 530 N. 15th St., Marquette Univ., Milwaukee, WI 53233 (e-mail: james.buchanan@marquette.edu).

REFERENCES

Antri M, Fénelon K, Dubuc R. The contribution of synaptic inputs to sustained depolarizations in reticulospinal neurons. ***J Neurosci*** *29*: 1140–1151, 2009.

Arshavsky YI, Berkinblit MB, Fukson OI, Gelfand IM, Orlovsky GN. Recordings of neurons of the dorsal spinocerebellar tract during evoked locomotion. ***Brain Res*** *43*: 272–275, 1972.

Arshavsky YI, Gelfand IM, Orlovsky GN, Pavlova GA. Messages conveyed by spinocerebellar pathways during scratching in the cat. I. Activity of neurons of the lateral reticular nucleus. ***Brain Res*** *151*: 479–491, 1978a.

Arshavsky YI, Gelfand IM, Orlovsky GN, Pavlova GA. Messages conveyed by spinocerebellar pathways during scratching in the cat. II. Activity of neurons of the ventral spinocerebellar tract. ***Brain Res*** *151*:493–506, 1978b.

Berry MS, Pentreath VW. Criteria for distinguishing between monosynaptic and polysynaptic transmission. ***Brain Res*** *105*: 1–20, 1976.

Brocard F, Ryczko D, Fénelon K, Hatem R, Gonzales D, Auclair F, Dubuc R. The transformation of a unilateral locomotor command into a symmetrical bilateral activation in the brainstem. ***J Neurosci*** *30*: 523–533, 2010.

Buchanan JT. Identification of interneurons with contralateral, caudal axons in the lamprey spinal cord: synaptic interactions and morphology. ***J Neurophysiol*** *47*: 961–975, 1982.

Buchanan JT. Contributions of identifiable neurons and neuron classes to lamprey vertebrate neurobiology. ***Prog Neurobiol*** *63*: 441–466, 2001.

Buchanan JT, Cohen AH. Activities of identified interneurons, motoneurons, and muscle fibers during fictive swimming in the lamprey and effects of reticulospinal and dorsal cell stimulation. ***J Neurophysiol*** *47*: 948–960, 1982.

Buchanan JT, Kasicki S. Activities of spinal neurons during brainstem-dependent fictive swimming in lamprey. ***J Neurophysiol*** *73*: 80–87, 1995.

Buchanan JT, Kasicki S. Segmental distribution of common synaptic inputs to spinal motoneurons during fictive swimming in the lamprey. ***J Neurophysiol*** *82*: 1156–1163, 1999.

Chong M, Drapeau P. Interaction between hindbrain and spinal networks during the development of locomotion in zebrafish. ***Dev Neurobiol*** *67*: 933–947, 2007.

Deliagina TG, Zelenin PV, Fagerstedt P, Grillner S, Orlovsky GN. Activity of reticulospinal neurons during locomotion in the freely behaving lamprey. ***J Neurophysiol*** *83*: 853–863, 2000.

Di Prisco GV, Pearlstein E, Le Ray D, Robitaille R, Dubuc R. A cellular mechanism for the transformation of a sensory input into a motor command. ***J Neurosci*** *20*: 8169–8176, 2000.

Di Prisco GV, Pearlstein E, Robitaille R, Dubuc R. Role of sensory-evoked NMDA plateau potentials in the initiation of locomotion. ***Science*** *278*: 1122–1125, 1997.

Drew T, Kalaska J, Krouchev N. Muscle synergies during locomotion in the cat: a model for motor cortex control. ***J Physiol*** *586*: 1239–1245, 2008.

Dubuc R, Brocard F, Antri M, Fénelon K, Gariépy JF, Smetana R, Ménard A, Le Ray D., Viana Di Prisco G, Pearlstein E, Sirota MG, Derjean D, St-Pierre M, Zielinski B, Auclair F, Veilleux D. Initiation of locomotion in lampreys. ***Brain Res Rev*** *57*: 172–182, 2008.

Dubuc R, Grillner S. The role of spinal cord inputs in modulating the activity of reticulospinal neurons during fictive locomotion in the lamprey. ***Brain Res*** *483*: 196–200, 1989.

Einum JF, Buchanan JT. Reticulospinal neurons receive direct spinobulbar inputs during locomotor activity in lamprey. ***J Neurophysiol*** *92*: 1384–1390, 2004.

Einum JF, Buchanan JT. Membrane potential oscillations in reticulospinal and spinobulbar neurons during locomotor activity. ***J Neurophysiol*** *94*: 273–281, 2005.

Einum JF, Buchanan JT. Spinobulbar neurons in lamprey: cellular properties and synaptic interactions. ***J Neurophysiol*** *96*: 2042–2055, 2006.

Fagerstedt P, Orlovsky GN, Deliagina TG, Grillner S, Ullen F. Lateral turns in the lamprey. II. Activity of reticulospinal neurons during the generation of fictive turns. ***J Neurophysiol*** *86*: 2257–2265, 2001.

Grillner S. Biological pattern generation: the cellular and computational logic of networks in motion. ***Neuron*** *52*:751–766, 2006.

Jackson AW, Horinek DF, Boyd MR, McClellan AD. Disruption of left-right reciprocal coupling in the spinal cord of larval lamprey abolishes brain-initiated locomotor activity. ***J Neurophysiol*** *94*: 2031–2044, 2005.

Kasicki S, Grillner S. Müller cells and other reticulospinal neurons are phasically active during fictive locomotion in the isolated nervous system of the lamprey. ***Neurosci Lett*** *69*: 239–243, 1986.

Kasicki S, Grillner S, Ohta Y, Dubuc R, Brodin L. Phasic modulation of reticulospinal neurons during fictive locomotion and other types of spinal motor activity in lamprey. ***Brain Res*** *484*: 203–216, 1989.

Li WC, Roberts A, Soffe SR. Locomotor rhythm maintenance: electrical coupling among premotor excitatory interneurons in the brainstem and spinal cord of young *Xenopus* tadpoles. ***J Physiol*** *587*: 1677–1693, 2009.

Li WC, Soffe SR, Wolf E, Roberts A. Persistent responses to brief stimuli: feedback excitation among brainstem neurons. ***J Neurosci*** *26*: 4026–4035, 2006.

Matsuyama K, Mori F, Nakajima K, Drew T, Aoki M, Mori S. Locomotor role of the corticoreticular-reticulospinal-spinal interneuronal system. ***Prog Brain Res*** *143*: 239–249, 2004.

Mullins OJ, Hackett JT, Buchanan JT, Friesen WO. Neuronal control of swimming behavior: comparison of vertebrate and invertebrate model systems. ***Prog Neurobiol*** *93*: 244–269, 2011.

Orlovsky GN. Work of the reticulospinal neurons during locomotion. ***Biophysics*** *15*: 761–771, 1970a.

Orlovsky GN. Influence of the cerebellum on the reticulospinal neurons during locomotion. ***Biophysics*** *15*: 928–936, 1970b.

Orlovsky GN, Deliagina TG, Grillner S. ***Neuronal Control of Locomotion: From Mollusc to Man***. Oxford, UK: Oxford University Press, 1999.

Perreault MC, Drew T, Rossignol S. Activity of medullary reticulospinal neurons during fictive locomotion. ***J Neurophysiol*** *69*: 2232–2247, 1993.

Ronan M. Origins of the descending spinal projections in petromyzontid and myxinoid agnathans. ***J Comp Neurol*** *281*: 54–68, 1989.

Ronan M, Northcutt RG. Projections ascending from the spinal cord to the brain in petromyontid and myxinoid agnathans. ***J Comp Neurol*** *291*: 491–508, 1990.

Rovainen CM. Physiological and anatomical studies on large neurons of central nervous system of the sea lamprey (*Petromyzon marinus*). I. Müller and Mauthner cells. ***J Neurophysiol*** *30*: 1000–1023, 1967.

Rovainen CM. Synaptic interactions of reticulospinal neurons and nerve cells in the spinal cord of the sea lamprey. ***J Comp Neurol*** *154*: 207–223, 1974.

Shaw AC, Jackson AW, Holmes T, Thurman S, Davis GR, McClellan AD. Descending brain neurons in larval lamprey: spinal projection patterns and initiation of locomotion. ***Exp Neurol*** *224*: 527–544, 2010.

Smetana R, Juvin L, Dubuc R, Alford S. A parallel cholinergic brainstem pathway for enhancing locomotor drive. ***Nat Neurosci*** *13*: 731–738, 2010.

Soffe SR, Roberts A, Li WC. Defining the excitatory neurons that drive the locomotor rhythm in a simple vertebrate: insights into the origin of reticulospinal control. ***J Physiol*** *587*: 4829–4844, 2009.

Swain GP, Snedeker JA, Ayers J, Selzer ME. Cytoarchitecture of spinal-projecting neurons in the brain of the larval sea lamprey. ***J Comp Neurol*** *336*: 194–210, 1993.

Vinay L, Bongianni F, Ohta Y, Grillner S, Dubuc R. Spinal inputs from lateral columns to reticulospinal neurons in lampreys. ***Brain Res*** *808*: 279–293, 1998a.

Vinay L, Bussières N, Shupliakov O, Dubuc R, Grillner S. Anatomical study of spinobulbar neurons in lampreys. ***J Comp Neurol*** *397*: 475–492, 1998b.

Wallén P, Grillner S, Feldman JL, Bergelt S. Dorsal and ventral myotome motoneurons and their input during fictive locomotion in lamprey. ***J Neurosci*** *5*: 654–661, 1985.

Wallén P, Williams TL. Fictive locomotion in the lamprey spinal cord in vitro compared with swimming in the intact and spinal animal. ***J Physiol*** *347*: 225–239, 1984.

Zar JH. ***Biostatistical Analysis*** (4th ed.). Upper Saddle River, NJ: Prentice-Hall, 1999.

Zelenin PV, Grillner S, Orlovsky GN, Deliagina TG. Heterogeneity of the population of command neurons in the lamprey. ***J Neurosci*** *21*: 7793–7803, 2001.

Zelenin PV, Orlovsky GN, Deliagina TG. Sensory-motor transformation by individual command neurons. ***J Neurosci*** *27*: 1024–1032, 2007.

Zottoli SJ, Cioni C, Seyfarth EA. Reticulospinal neurons in anamniotic vertebrates: a celebration of Alberto Stefanelli's contributions to comparative neuroscience. ***Brain Res Bull*** *74*: 295–306, 2007.